Cancer Chemother Pharmacol (1989) 24: 354–358

Cancer Chemotherapy and Pharmacology

Metabolism and pharmacokinetics of *p*-(3,3-dimethyl-1-triazeno) benzoic acid in M5076 sarcoma-bearing mice

Emilio Benfenati, Pierluigi Farina, Tina Colombo, Gianluca De Bellis, Mauro Valerio Capodiferro, and Maurizio D'Incalci

Istituto di Ricerche Farmacologiche "Mario Negri", Via Eritrea 62, 20157 Milano, and Laboratori Negri Bergamo, Via Gavazzeni 11, I-24100 Bergamo, Italy

Summary. The pharmacokinetics of the anticancer agent *p*-(3,3-dimethyl-1-triazeno) benzoic acid (pCOOH-DMT), a drug now in phase I clinical trial in Europe, was investigated in C57Bl female mice with M5076 reticulum-cell sarcoma that were treated i.v. with 200 mg/kg pCOOH-DMT. The drug disappeared from plasma with a terminal half-life of about 2.5 h. Plasma clearance was approximately 6 ml/min per kg. Distribution studies showed some differences in drug levels in different tissues. The highest levels were found in the tumor, liver, kidney and lung; lower levels were found in the spleen and gut, and the lowest, in the brain. The *N*-desmethyl derivative of pCOOH-DMT was not detectable in plasma or tissues of mice treated with the drug. Therefore, the previous evidence of low *N*-demethylation of pCOOH-DMT was confirmed. pCOOH-DMT glucuronide was identified by mass spectrometry and quantified by high-performance liquid chromatography (HPLC) in plasma, tissues and urine samples. pCOOH-DMT glucuronide appears to be the major urinary metabolite of pCOOH-DMT in mice. Another metabolite identified by mass spectrometry and quantified by HPLC in some tissues and urine was pCOOH-DMT glycinate.

Introduction

5-(3,3-Dimethyl-1-triazeno)imidazole-4-carboxamide (DTIC) is an anticancer agent that has been used for many years for the therapy of melanoma and lymphomas [2]. In an attempt to find more effective and less toxic analogs, many aryldimethyltriazenes have been synthesized and tested [1] for their antineoplastic activity in mice. One of them, *p*-(3,3-dimethyl-1-triazeno)benzoic acid (pCOOH-DMT) [10], appears to have greater antimetastatic [9, 14] and antitumor activity in some murine tumors [5, 6] and less toxicity than DTIC; therefore, it has been selected for phase I clinical trials [4]. To obtain information on the metabolism and pharmacokinetics of pCOOH-DMT, we developed a specific high-performance liquid chromatographic (HPLC) assay [7] for this drug and its probable metabolites in biological fluids and tissues. Using this method, we investigated the metabolism and pharmacokinetics of pCOOH-DMT in mice bearing M5076 reticulum-cell sarcoma, a tumor that is sensitive to the drug [5, 6]. We also report the identification by HPLC and mass spectrometry (MS) of the two major metabolites occurring in plasma, urine and tissues.

Abbreviations: DTIC, 5-(3,3-dimethyl-1-triazeno)imidazole-4-carboxamide; pCOOH-DMT, *p*-(3,3-dimethyl-1-triazeno)benzoic acid; pCOOH-MMT, *p*-(3-methyl-1-triazeno)benzoic acid; $pCONH_2$-DMT, *p*-(3,3-dimethyl-1-triazeno)carboxamide; BSTFA, *N,O*-bis(trimethylsilyl)trifluoroacetamide; TMCS, trimethylchlorosilane; TLC, thin-layer chromatography; FAB, fast atom bombardment; EI, electron impact; M5, M5076 reticulum-cell sarcoma; $t_{1/2}\beta$, beta-half-life; C_o, concentration time 0; AUC, area under the concentration vs time curve; Cl, total clearance; V_β, volume of distribution

Offprint requests to: Maurizio D'Incalci

Materials and methods

Chemicals. pCOOH-DMT glycinate was kindly supplied by Dr. D. E. V. Wilman (Institute of Cancer Research, CRC Laboratory, Surrey, UK). All other triazenes were kindly supplied by Prof. C. Nisi (Trieste, Italy), who synthesized them according to previously published methods [10]. Stock solutions were prepared in methanol every 2 weeks and stored at −20° C. For pharmacokinetic and metabolic studies, pCOOH-DMT (potassium salt) was dissolved in saline immediately before its administration to mice. The structure of pCOOH-DMT is shown in Fig. 1. Ammonium sulphate and *N*-(1-naphthyl)-ethylenediammonium dichloride were obtained from E. Merck (Darmstadt, FRG). *N,O*-bis(trimethylsilyl)trifluoroacetamide (BSTFA) and trimethylchlorosilane (TMCS) were obtained from Pierce Chemical Company (Rockford, Ill). β-Glucuronidase was obtained from Boehringer (Mannheim, FRG).

Animals and tumors. Female C57BL/6J mice (mean weight, 20 ± 2 g) obtained from Charles River Laboratories, Italy, received an i.m. transplant of 5×10^5 M5076 ovarian reticulum-cell sarcoma (M5) cells supplied by Mason Research Institute (DTC – Animal and Human Tumor Bank, Worcester, Mass). For the determination of the plasma and tissue kinetics of pCOOH-DMT, the drug was dissolved in saline and injected i.v. at a dose of

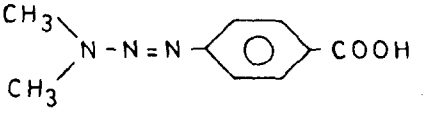

Fig. 1. Structure of pCOOH-DMT

200 mg/kg into M5-bearing mice 15 days after tumor implantation. At various times after injection (1, 5, 15, 30, 60, 120, 240, 360 and 480 min), three animals per respective time point were killed and plasma and tissues (tumor, brain, lung, liver, spleen, kidney and small intestine) were taken, gently washed in cold saline (4° C), dried on filter paper and stored at −20° C until analysis. One group of M5-bearing mice (five animals) was housed in metabolic cages until 72 h after drug administration. Urine samples were collected at different intervals (0–6 h, 6–24 h, 24–48 h, 48–72 h) and immediately stored at −20° C until analysis.

Analytical assay. The plasma HPLC assay for triazenes, described in detail elsewhere [7] can be summarized as follows: tissues homogenized in water (1:4, w/v), plasma and urine samples were deproteinized with two equivalent volumes of ice-cold methanol and mixed in a vortex for 30 s. Samples were cooled to −60° C using acetone and dry ice for 2 min and centrifuged, and the clear methanolic solution was injected directly onto the HPLC column. $pCONH_2$-DMT was added as the internal standard. Separation was carried out on a Waters model 440 instrument equipped with a 340-nm adsorbance detector. An isocratic solvent system of 0.005 *M* tetrabutylammonium hydroxide in bidistilled water (buffered at pH 7.6 with phosphoric acid) and acetonitrile (82:18, v/v) was delivered at the rate of 1.5 ml/min using a 25-cm-long (inside diameter, 4 mm) LiChrosorb RP18 (10 µm) column (Merck, Darmstadt, FRG). Recovery of pCOOH-DMT and pCOOH-DMT glycinate was 89%±4% in plasma and urine and 85%±3% in tissues. The limit of sensitivity for pCOOH-DMT was 0.5±0.05 nmol/ml plasma and urine and 1±0.1 nmol/g tissue.

The calibration curve for pCOOH-DMT glycinate was linear ($r = 0.99$) from 0.5 to 5 nmol/ml urine; it had a slope of 0.07 and an intercept of 0.055. The limit of sensitivity for this metabolite was 0.5 nmol/ml urine. Considering all the values of calibration curves for pCOOH-DMT and pCOOH-DMT glycinate, that were done on different days during 3 months of study, we found that the maximal coefficient of variation was 11%.

Thin-layer chromatography. Mouse urine was analyzed by thin-layer chromatography (TLC) on silica gel 60F-254 plates (E. Merck, Darmstadt, FRG); acetone-ethyl acetate-water (4/1/1, by vol.) was used as the eluent. A portion of the plate was sprayed with *N*-(1-naphthyl)-ethylenediammonium dichloride, a specific reagent for the detection of triazenes [11]. The isolated compounds were scraped off the TLC plate, dissolved in acetone-water (1/9, v/v), dried under a nitrogen stream, redissolved in acetone-water (1/1, v/v), redried under a nitrogen stream and analyzed by mass spectrometry. Co-chromatography with authentic samples of pCOOH-DMT and pCOOH-DMT glycinate was also done.

Mass spectrometry. Electron impact (EI) mass spectra were determined with a VG 70–250 mass spectrometer (VG Analytical, Manchester, UK) by the direct inlet system. The electron energy was 20 eV. Fast atom bombardment (FAB) mass spectra were acquired using a VG 70–250 mass spectrometer, equipped with its standard FAB source operating at 8 kV. Glycerol was used as a matrix and xenon was the bombarding gas. The analyses were carried out at room temperature and 6 kV accelerating voltage.

Pharmacokinetic analysis. Plasma and tissue data were fitted using a general nonlinear fitting program running on a microcomputer [13], minimizing the sum of squared errors. The beta-half-life ($t_{½}\beta$), total clearance (Cl), and volume of distribution (V_β) were computed as follows: $t_{½}\beta = 0.693/\beta$; Cl = dose/AUC; $V_\beta = Cl/\beta$. C_o was the concentration extrapolated at time 0, whereas the peak levels were the experimentally determined maximal concentrations. The AUC (nmol/ml or g × min) was calculated by the trapezoidal rule, extrapolating from the last sampling time to infinity with the formula

$$\int \infty C^{*\,C(t)dt} = C^*/\beta,$$

where C* is the plasma or tissue concentration measured at the last time point.

Results

Distribution of pCOOH-DMT

Table 1 shows the main pharmacokinetic parameters of pCOOH-DMT after i.v. doses of 100 or 200 mg/kg. The drug disappeared from plasma with a biexponential decay. Clearance values were similar after both doses. Figure 2 shows plasma and tissue levels of pCOOH-DMT at different intervals after the i.v. injection of 200 mg/kg in M5 reticulum-cell-sarcoma-bearing mice. Table 2 shows the peak levels and AUC values of pCOOH-DMT in plasma and different tissues. pCOOH-DMT levels varied in different tissues. In the tumor, liver, kidney and lung, relatively high levels were found; lower levels were found in the spleen and gut, and the lowest, in the brain. The 72-h cumulative urinary excretion of pCOOH-DMT as unchanged drug corresponded to approximately 0.5% of the delivered dose (200 mg/kg).

Table 1. Plasma pharmacokinetic parameters of pCOOH-DMT after 100 and 200 mg/kg i.v.

Dose (mg/kg)	$T_{1/2}\beta$ (min)	C_o (µmol/ml)	AUC (µmol/ml × min)	Cl (ml/min/kg)	V_β (l/kg)
100	157	1.58	81	6.4	1.46
200	146	2.95	177	5.8	1.24

For details see *Materials and methods*

Table 2. Plasma and tissue levels of pCOOH-DMT after 200 mg/kg i.v.

	Peak level (µmol/ml or g±SE)	AUC (µmol/ml or g × min)
Plasma	4.52±0.46	174.2
Tumor	1.15±0.1	93.3
Liver	1.58±0.1	83.9
Small intestine	1.11±0.1	38.8
Kidney	1.44±0.2	69.7
Spleen	0.64±0.04	33.4
Lung	2.47±0.5	82.8
Brain	1.11±0.3	28.4

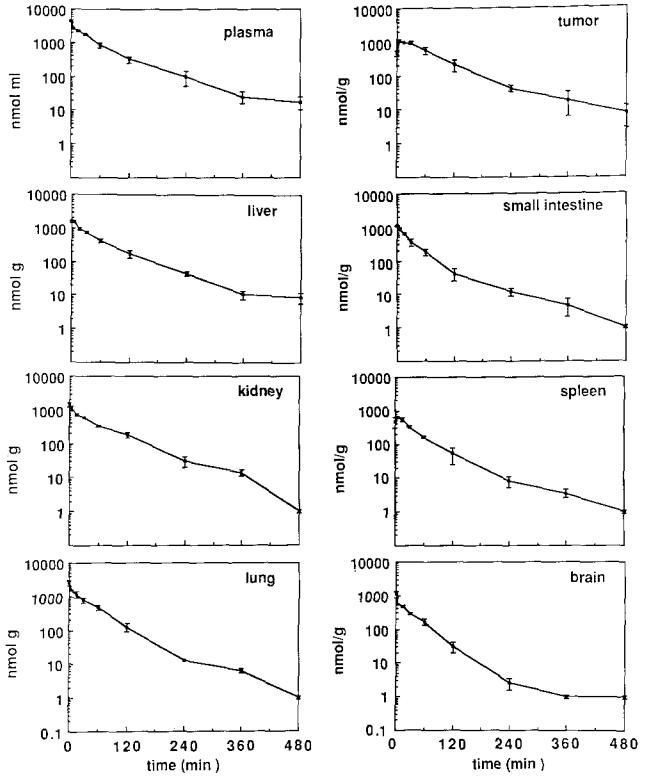

Fig. 2. Kinetics of pCOOH-DMT concentration in plasma and tissues (mean of three animals per time point)

Identification of the metabolites as pCOOH-DMT glucuronide and pCOOH-DMT glycinate

Under the HPLC conditions described, in addition to the peaks corresponding to pCOOH-DMT and the internal standard ($pCONH_2$-DMT) in plasma, urine and most tissue extracts, we observed two other peaks with retention times of 7.7 and 9.4 min (for example, see the chromatogram of urinary extract 6 h after 200 mg/kg pCOOH-DMT; Fig. 3). The HPLC retention times of these metabolites were different from that of 1-*p*-(3-methyl-1-triazeno)-benzoic acid (pCOOH-MMT), the *N*-desmethyl derivative of pCOOH-DMT, which was 4 min. Under our laboratory conditions, the pCOOH-MMT peak was never seen in chromatograms of the extracts analyzed. By using HPLC separation, we repeatedly collected the fraction corresponding to the unknown metabolites and concentrated it by freeze-drying. Mass spectrometry (MS) was used to identify the metabolites.

We derived metabolite I using BSTFA and TMCS in pyridine. The EI mass spectrum of the silylated metabolite is reported in Fig. 4; it presents a molecular ion at m/z 657, corresponding to the silylated glucuronide of pCOOH-DMT. The ion at m/z 217 is attributable to the silylated glucuronide moiety [3]. The base peak at m/z 176 is probably due to the loss of the glucuronic group through cleavage of the acyl-oxygen bond. The ion at m/z 147 $(Me_3Si\text{-}O = SiMe_2)^+$ is common to silylated polyols [12].

For further evidence, we analyzed this extract sample with FAB MS. Figure 5a shows the FAB mass spectrum of the metabolite. A pseudo-molecular ion at m/z 414 is very probably attributable to the addition of 2Na to the glucuronide of pCOOH-DMT ($MNa^+ + Na - H$). The ion at m/z 238 (the base peak) probably originated from the

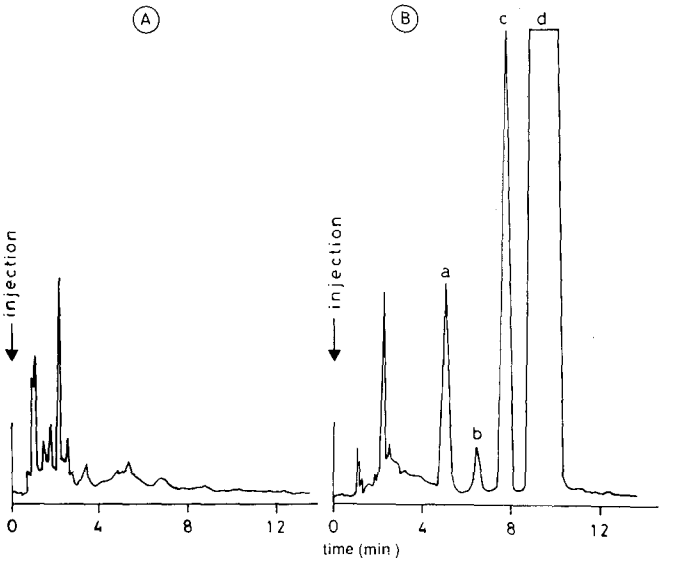

Fig. 3. HPLC chromatogram of mouse urinary extract before (*panel A*) and after treatment with pCOOH-DMT (*panel B*). Urine samples were collected between 0 and 6 h after an i.v. dose of 200 mg/kg. Peaks *a, b, c and d* are due to the internal standard ($pCONH_2$-DMT), pCOOH-DMT, metabolite II and metabolite I, respectively

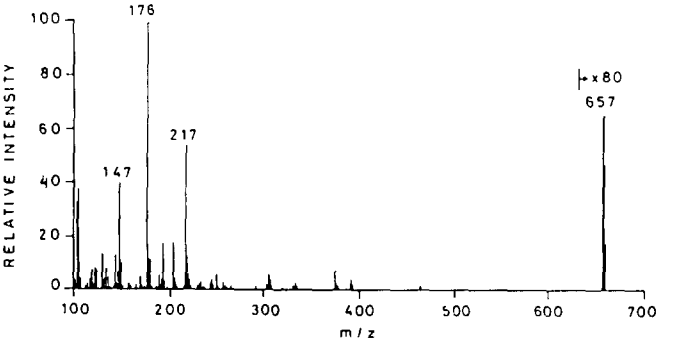

Fig. 4. The EI mass spectrum of pCOOH-DMT metabolite I (glucuronide) after derivation

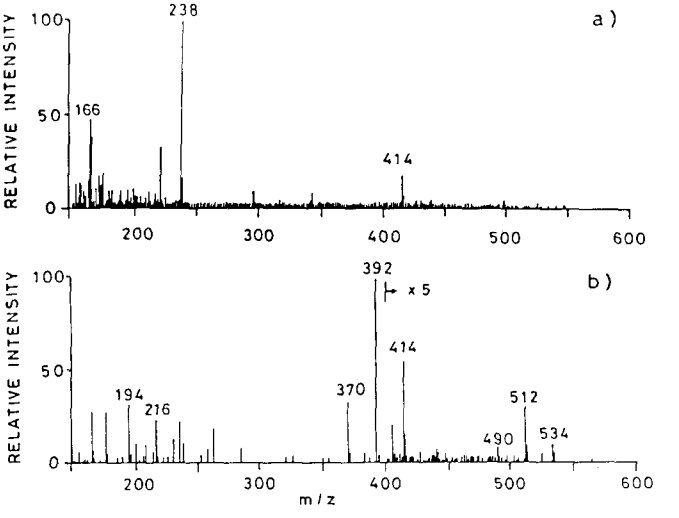

Fig. 5.a The FAB mass spectrum of the pCOOH-DMT glucuronide. **b** As in **a** after the addition of ammonium sulphate

pCOOH-DMT group + 2Na − H. Similarly, the ion at m/z 166 could be due to the benzoyl moiety + 2Na − H.

To shift these ions and confirm this interpretation, we added ammonium sulphate to the metabolite, obtaining the spectrum reported in Fig. 5b. A peak appeared at m/z 370, corresponding to the protonated molecular ion of the glucuronide; the occurrence of this peak strongly supports the identification of the metabolite as the glucuronide. The ion at m/z 392 (base peak) is due to the $(M+Na)^+$ species. A new peak appeared at m/z 490, corresponding to the adduct $(MH + NaHSO_4)^+$; this cluster ion is further evidence of the proposed structure for the metabolite. The ions at m/z 512 and 534 are the adducts $(M + Na + NaHSO_4)^+$ and $(M + 2Na + NaHSO_4 - H)^+$, respectively. The ions appeared at m/z 194 (pCOOH-DMT + H)$^+$ and at m/z 216 (pCOOH-DMT + Na)$^+$, which confirms that the metabolite is the glucuronide.

In addition, when biological samples (e.g. urine) were incubated overnight at 37° C with β-glucuronidase, the pCOOH-DMT glucuronide peak disappeared with a corresponding increase in the peak of pCOOH-DMT. The retention time of metabolite II corresponds to the glycinate, and its mobility on TLC was also identical to that of the glycinate. We further confirmed its identity on the basis of its FAB mass spectrum. The positive FAB spectrum of standard glycinate presents the $(M + H)^+$ peaks at m/z 251; a negative FAB spectrum shows $(M - H)^-$ at m/z 249. Positive and negative FAB spectra of the second metabolite presented the typical ions of glycinate, confirming the characterization on the basis of its chromatographic behavior.

Kinetics of pCOOH-DMT glucuronide and pCOOH-DMT glycinate

Figure 6 illustrates the kinetics of pCOOH-DMT glucuronide in the plasma, small intestine, liver, kidney and lung of M5 tumor-bearing mice after the i.v. administration of 200 mg/kg pCOOH-DMT. Since we did not have the standard for pCOOH-DMT glucuronide, we could not estimate the absolute concentrations of this metabolite; the data are therefore given in nmol equivalents, assuming the same extinction coefficient for pCOOH-DMT glucuronide and pCOOH-DMT.

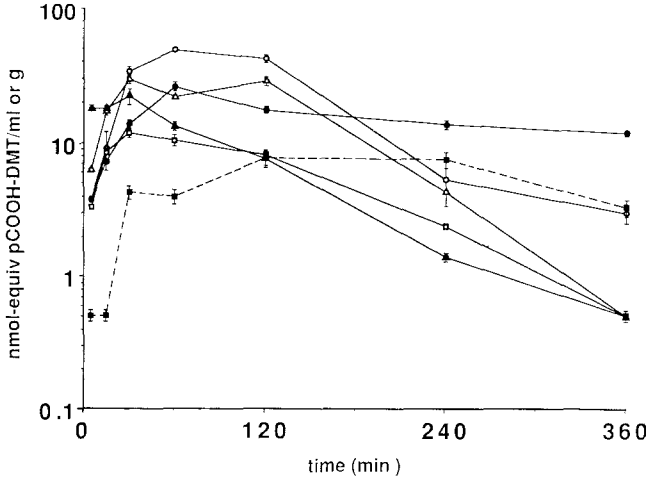

Fig. 6. Kinetics of pCOOH-DMT glucuronide in plasma (○), small intestine (●), liver (▲), kidney (△) and lung (□) after an i.v. dose of 200 mg/kg pCOOH-DMT. The *dotted line* represents the kinetics of pCOOH-DMT glycinate in the small intestine (mean of three animals per time point)

In plasma, pCOOH-DMT glucuronide reached a maximum 60 min after drug injection, then started slowly to decline. The concentration of this metabolite in the 2 h following drug injection was relatively high in several tissues, in some cases being similar to those found in plasma (e.g. small intestine and kidney). The level of the glucuronide disappeared rapidly from all of these tissues except the small intestine, where the levels were still high at 360 min. In the tumor, spleen and brain, the levels of pCOOH-DMT glucuronide were negligible. In urine (collected for 72 h after drug treatment), the cumulative excretion of the glucuronide corresponded to approximately 4% of the delivered dose.

pCOOH-DMT glycinate was not detectable in plasma or in any of the other tissues analyzed except the kidney and small intestine. In the kidney, however, these concentations were too low for a quantitative determination (≤ 1 nmol/g). The kinetics of this metabolite in the small intestine is illustrated in Fig. 6 (*dotted line*). The 72-h urinary excretion was 2.5% of the delivered dose.

Discussion

Although pCOOH-DMT is now undergoing phase I trial, no published information is available on the biotransformation pattern or kinetics of this drug in animals. Using a specific HPLC assay [7], we investigated the pharmacokinetics of pCOOH-DMT in M5076 reticulum-cell-sarcoma-bearing mice receiving the drug i.v. pCOOH-DMT disappears from plasma biphasically, with a terminal half-life of 2.5 h. Plasma clearance was approximately 6 ml/min per kg after doses of 100 or 200 mg/kg. Plasma levels were higher than tissue levels.

Interesting differences were observed among the various tissues tested. Drug levels in the tumor were relatively high and long-lasting, still being measurable 8 h after the i.v. administration of 200 mg/kg. In the live, which is the main site of M5 metastasis, relatively high concentrations were found. pCOOH-DMT concentrations were also high in the lung, which is the site of metastatic involvement of Lewis lung carcinoma, a mouse tumor that is particularly sensitive to the antimetastatic activity of this drug [9, 14]. The lowest drug AUC values were found in the brain, where pCOOH-DMT reached high concentrations just after injection but was cleared very rapidly, being undetectable by 6 h after treatment.

The mechanism of action of pCOOH-DMT is unknown. However, it is generally assumed that dimethyltriazenes require metabolic activation with the formation of *N*-demethylated metabolites, which are potent alkylating agents [17]. If this also holds true for pCOOH-DMT, the distribution data of the parent compound (e.g. pCOOH-DMT tumor levels) may be unimportant in relation to the activity of the drug, the concentrations of the active metabolites being much more important.

However, pCOOH-DMT appears to differ somewhat from other triazenes. Previous work has in fact shown that the 9,000 *g* mouse-liver fraction produces *N*-demethylation of pCOOH-DMT much less efficiently than other dimethyltriazenes with similar structures [15, 16]. For example, Farina et al. [7] reported that after an 80-min incuba-

tion with 9,000 *g* mouse-liver fraction and NADPH, only 24% of pCOOH-DMT was metabolized, compared with 79% of *p*-(3,3-dimethyl-1-triazeno)acetophenone. In addition, after treatment with *p*-(3,3-dimethyl-1-triazeno)acetophenone, the N-desmethyl metabolite was present at appreciable concentrations in mouse plasma. In contrast, pCOOH-MMT was undetectable in plasma or tissues of mice treated with pCOOH-DMT when the sensitivity of the assay was 0.5 nmol/ml in plasma or about 1 nmol/g in tissues. The low *N*-demethylation rate of pCOOH-DMT [7, 15, 16] argues against the hypothesis that pCOOH-MMT is responsible for pCOOH-DMT's antitumor activity.

pCOOH-DMT undergoes conjugation with glucuronic acid and glycine. MS studies provide unequivocal evidence that pCOOH-DMT glucuronide is present in urine, plasma and some tissues of mice treated i.v. with pCOOH-DMT. MS studies also confirm the presence of pCOOH-DMT glycinate in the urine and small intestine of these animals. Although the lack of a standard made an absolute quantification of pCOOH-DMT glucuronide impossible, it is certainly the major urinary metabolite of pCOOH-DMT. Clearance of pCOOH-DMT from the body is likely to be greatly influenced by the formation and elimination of these metabolites, which have also been recently found in large amounts in the urine of cancer patients receiving pCOOH-DMT in phase I clinical trials [4, 8].

Acknowledgements. This work was supported by CNR (Rome, Italy) Project Oncology contracts 87.01526.44 and 88.00644.44. The generous contribution of the Italian Association for Cancer Research (Milan, Italy) is gratefully acknowledged. This work was done in the frame of the activities of the Pharmacokinetics and Metabolism Group (PAM) of the EORTC and benefited from the exchange of reagents and ideas and fruitful discussions between active members of the group.

References

1. Audette RCS, Connors TA, Mandel HG, Merai K, Ross WCJ (1973) Studies on the mechanism of action of the tumor inhibitory triazenes. Biochem Pharmacol 22: 1855
2. Beretta G, Bonadonna G, Bajetta E, Tancini G, De Lena M, Azzarelli A, Veronesi U (1976) Combination chemotherapy with DTIC (NSC-45388) in advanced malignant melanoma, soft tissue sarcomas, and Hodgkin's disease. Cancer Treat Rep 60: 205
3. Billets S, Lietman PS, Fenselau C (1973) Mass spectral analysis of glucuronides. J Med Chem 16: 30
4. CB 10-277 (1988) EORTC newsletter 165. EORTC, London Newcastle, p 6
5. Colombo T, D'Incalci M (1984) Comparison of the antitumor activity of DTIC and 1-*p*-(3,3-dimethyl-1-triazeno)benzoic acid potassium salt on murine transplantable tumors and their hematological toxicity. Cancer Chemother Pharmacol 13: 139
6. Colombo T, Garattini S, Lassiani L, D'Incalci M (1982) Activity of 1-*p*-(3,3-dimethyl-1-triazeno)benzoic acid potassium salt in M5076/73A ovarian reticular cell sarcoma of the mouse. Cancer Treat Rep 66: 1945
7. Farina P, Benfenati E, Lassiani L, Nisi C, D'Incalci M (1985) High-performance liquid chromatographic assay for the determination of *p*-(3,3-dimethyl-1-triazeno)benzoic acid in mouse plasma. J Chromatogr 345: 323
8. Foster BJ, Mewell DR, Carmichael J, Harris AL, Gumbrell LA, Wilman DEV, Calvert AH (1988) Preclinical and clinical pharmacokinetic studies with 1-(4-carboxyphenyl)-3,3-dimethyl triazene (CB10-277). Presented at the meeting on Modern anticancer drug development: molecules to man, Cambridge, December 14–17 (Abstract P7)
9. Giraldi T, Sava G, Cuman R, Nisi C, Lassiani L (1981) Selectivity of the antimetastatic and cytotoxic effects of 1-*p*-(3,3-dimethyl-1-triazeno)benzoic acid potassium salt, (±)-1,2-di(3,5-dioxopiperazin-1-yl)propane, and cyclophosphamide in mice bearing Lewis lung carcinoma. Cancer Res 41: 2524
10. Kolar GF (1972) Synthesis of biologically active triazenes from isolable diazonium salts. Z Naturforsch [B] 27: 1183
11. Loo TL, Stasswender EA (1967) Colorimetric determination of dialkyltriazenoimidazoles. J Pharm Sci 56: 1016
12. Pierce AE (1968) Silylation of organic compounds. A technique for gas-phase analysis. Pierce Chemical Co, Rockford, Illinois
13. Sacchi Landriani G, Guardabasso V, Rocchetti M (1983) NL-FIT: A microcomputer program for non-linear fitting. Comput Methods Programs Biomed 16: 35
14. Sava G, Giraldi T, Lassiani L, Nisi C (1979) Mechanism of the antimetastatic action of dimethyltriazenes. Cancer Treat Rep 63: 93
15. Sava G, Giraldi T, Lassiani L, Nisi C (1982) Metabolism and mechanism of the antileukemic action of isomeric aryldimethyltriazenes. Cancer Treat Rep 66: 1751
16. Sava G, Zorzet S, Perrisin L, Giraldi T, Lassiani L (1988) Effects of an inducer and an inhibitor of hepatic metabolism on the antitumor action of dimethyltriazenes. Cancer Chemother Pharmacol 21: 241
17. Vaughan K, Stevens MFG (1978) Monoalkyltriazenes. Chem Soc Rev 7: 377

Received 11 May 1988/Accepted 10 April 1989